ACS Chemical Neuroscience

Article

Synthesis and evaluation of a new ^{18}F-labeled radiotracer for studying the GABA$_A$ receptor in the mouse brain

Ravi Naik, Heather Valentine, Robert F. Dannals, Dean F Wong, and Andrew G. Horti

ACS Chem. Neurosci., **Just Accepted Manuscript** • DOI: 10.1021/acschemneuro.8b00038 • Publication Date (Web): 02 Mar 2018

ACS Publications

ACS Chemical Neuroscience is published by the American Chemical Society. 1155 Sixteenth Street N.W., Washington, DC 20036

Synthesis and evaluation of a new ^{18}F-labeled radiotracer for studying the $GABA_B$ receptor in the mouse brain

Ravi Naik[†], Heather Valentine[†], Robert F. Dannals[†], Dean F. Wong[†], Andrew G. Horti[†*]

[†]*Department of Radiology, The Johns Hopkins University School of Medicine, Baltimore, 21287 USA.*

ABSTRACT:

New $GABA_B$ agonists, fluoropyridyl ether analogues of baclofen, have been synthesized as potential PET radiotracers. The compound with highest inhibition binding affinity as well as greatest agonist response, (*R*)-4-amino-3-(4-chloro-3-((2-fluoropyridin-4-yl)methoxy)phenyl)butanoic acid (**1b**), was radiolabeled with ^{18}F with good radiochemical yield, high radiochemical purity, and high molar radioactivity. The regional brain distribution of the radiolabeled (*R*)-4-amino-3-(4-chloro-3-((2-[^{18}F]fluoropyridin-4-yl)methoxy)phenyl)butanoic acid, [^{18}F]**1b**, was studied in CD-1 male mice. The study demonstrated that [^{18}F]**1b** enters the mouse brain (1% ID/g tissue). The accumulation of [^{18}F]**1b** in the mouse brain was inhibited (35%) by pre-injection of $GABA_B$ agonist **1a** suggesting that the radiotracer brain uptake is partially mediated by $GABA_B$ receptors. The presented data demonstrated a feasibility of imaging of $GABA_B$ receptors in rodents and justify further development of $GABA_B$ PET tracers with improved specific binding and greater blood-brain barrier permeability.

Keywords: $GABA_B$ receptor, PET, radiotracer, autism, blood-brain barrier permeability

INTRODUCTION

$GABA_B$ is a receptor subclass for the neurotransmitter GABA (4-aminobutanoic acid).[1] Recent reviews summarize evidence that $GABA_B$ receptors play an essential role in various central and peripheral disorders.[2, 3] Molecules that modulate $GABA_B$ receptors are of great medicinal interest for the treatment of many disorders and conditions including alcohol dependence, anti-nociception, spasticity,

fragile X syndrome, Austin's disease, retinal ganglion cell degeneration, and autism.[4–9] The $GABA_B$ agonist baclofen **1** is widely used in the treatment of gastroesophageal reflux, cancer pain, and overactive bladder. Baclofen is under development for the treatment of behavioral symptoms of Fragile X Disorder.[4,10]

Autism is a neurodevelopmental disorder characterized by impairments in social interaction, restricted and repetitive behavior, and deficits in language and communication.[11] In 2006, in the USA and Europe a prevalence rate of autism of 116 per 10,000 children has been reported.[12]

Existing therapeutic agents are not effective for treatment of core symptoms of autism spectrum disorders.[13] Recent pre-clinical studies demonstrated that $GABA_B$ receptor agonist reverses social deficits and reduces repetitive behavior in animal models of autism.[14] Post-mortem studies have demonstrated that $GABA_B$ receptors are reduced (42-79%) in the various brain regions of subjects suffering from autism.[15]

Many $GABA_B$ drugs are analogues of GABA. These analogues are polar compounds that exhibit moderate BBB permeability. The recently developed baclofen derivative **1a** (Fig. **1**) demonstrated an improved BBB permeability and exhibited at least an order of magnitude higher $GABA_B$ receptor potency as compared to an active enantiomer of baclofen, R-(-)-baclofen (*R*-**1**) (pEC_{50} = 8.5 and 7.1, respectively).[4]

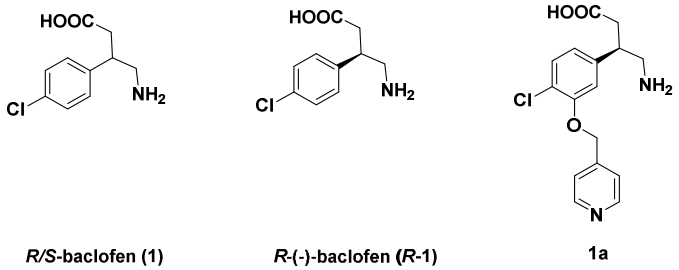

Figure 1. Structure of R-(-)-baclofen (*R*-**1**) and potent brain-penetrating $GABA_B$ agonist **1a**[4].

In vivo imaging and quantification of $GABA_B$ binding in the human brain would provide a significant advance in the understanding of autism and other $GABA_B$-related CNS disorders and could also facilitate

novel $GABA_B$ drug development. Positron emission tomography (PET) is the advanced technique to quantify neuronal receptors and their occupancy *in vivo*. Development of a suitable PET radiotracer for $GABA_B$ would be of substantial interest. Previously synthesized PET radiotracers **2-4** [16-18] (Fig. **2**) for imaging $GABA_B$ have shown negligible permeability of the blood-brain barrier (BBB) in animal experiments.

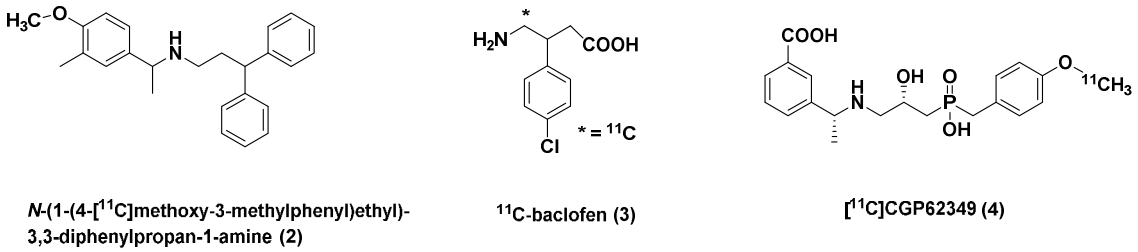

N-(1-(4-[^{11}C]methoxy-3-methylphenyl)ethyl)-3,3-diphenylpropan-1-amine (2)

^{11}C-baclofen (3)

[^{11}C]CGP62349 (4)

Figure 2. Previously reported $GABA_B$ PET radiotracers.

In this report, we describe the design, synthesis, ^{18}F-radiolabeling, and *in vitro* and *in vivo* characterization in mice of fluoro derivatives of **1a** as potential probes for PET imaging of $GABA_B$ receptors.

RESULTS AND DISCUSSION

Chemistry:

Compound **1a** was initially prepared as described elsewhere (Scheme **1**)[4]. However, the conversion of the intermediate iodo compound **9** to phenol **10** under the published conditions[4] afforded very low yield that is a common problem with the Suzuki reaction when an *ortho*-substituent is present.[19] Therefore, we designed a different methodology for the synthesis of the desired compound **10** (Schemes **2** and **3**).

This route started with protection of 4-chloro-3-hydroxybenzaldehyde **13** by using benzyl bromide in the presence of an inorganic base and DMF. The Henry reaction of a 3-(benzyloxy)-4-chlorobenzaldehyde **14** with nitromethane was used to give the nitrovinyl derivative **15** in good yields.

Next, a Michael reaction of compound **15** using (*R*)-3-acetyl-4-benzyloxazolidin-2-one **12** in the presence of NaHDMS gave the intermediate **16**.

Reduction of the nitro group of compound **16** followed by cyclization of the resulting amine *in situ* yielded **17** over two steps.[20, 21] Protection of lactam **17** with *t*-BOC gave the N-BOC derivative **18**. Debenzylation of **18** with palladium hydroxide gave the desired phenol **10** as a key intermediate. The intermediate **12** was synthesized from commercially available (*R*)-4-benzyloxazolidin-2-one **11** by using *n*-BuLi and acetyl chloride in THF (Scheme **2**).

The phenol **10** reacted with pyridyl alcohol *via* a modified Mitsunobu[22] reaction to give ether derivatives **19a-c** in high yields. The protected lactam **19a-c** underwent acidic hydrolysis to give the desired amino acid derivatives **1b-d** as shown in Scheme **3**.

Scheme 1. Synthesis of compound **1a.**

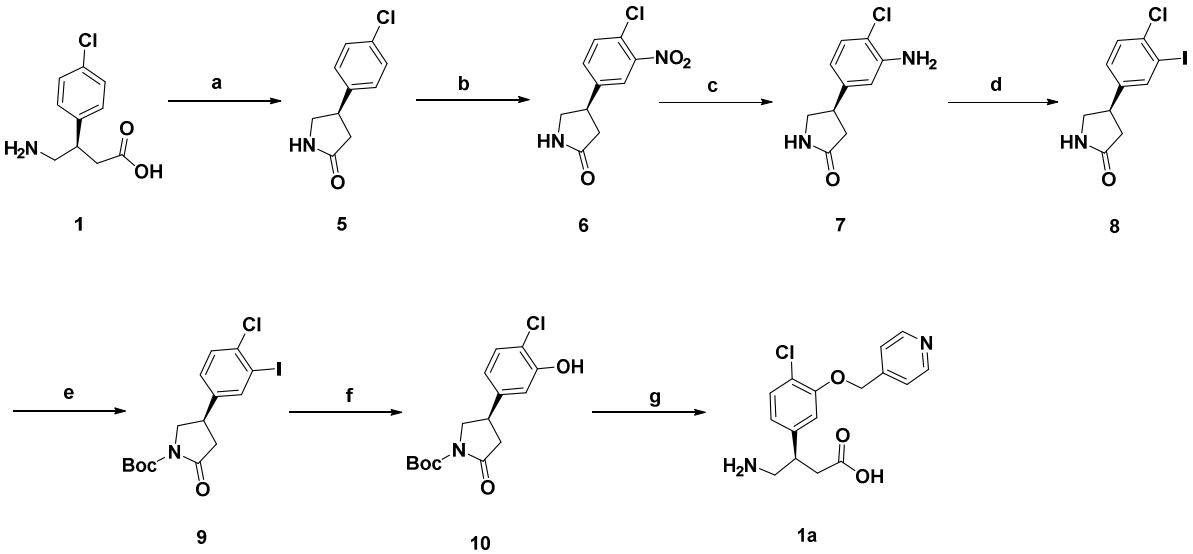

Reagents and conditions: (a) Acetic acid, reflux, 12h, 99%; (b) Guanidine nitrate, H_2SO_4, 0 °C to rt, 1h, 95%; (c) Zn, NH_4Cl, THF/MeOH/H_2O, reflux, 1h, 97%; (d) $NaNO_2$, KI, 12 N HCl, 0 °C to rt, 2.5 h, over three steps, 82%; (e) Boc anhydride, K_2CO_3, MC, rt, 12h, 92%; (f) (i) $PdCl_2(dppf)_2$, octamethyl 2,2-bis-1,3,2-dioxaborolane, KOAc, DMSO, 120 °C, 12h; (ii) 35% H_2O_2, DCM, 12h, over two steps, 17%; (g) i)

4-(bromomethyl)pyridine hydrobromide, K_2CO_3, Ethanol, 100 °C to rt, 12h, ii) 6N HCl, 90 °C to rt, 3h, over two steps, 69%.

Scheme 2. Synthesis of (*R*)-3-acetyl-4-benzyloxazolidin-2-one.

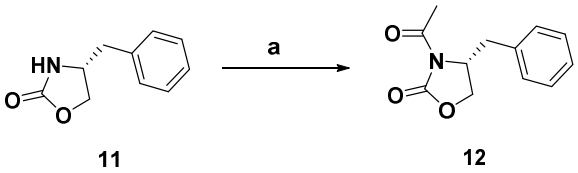

Reagents and conditions: (a) *n*-BuLi, Acetyl chloride, THF, -78 °C to rt, 4h, 89%.

Scheme 3. Synthesis of compounds **1b-d**.

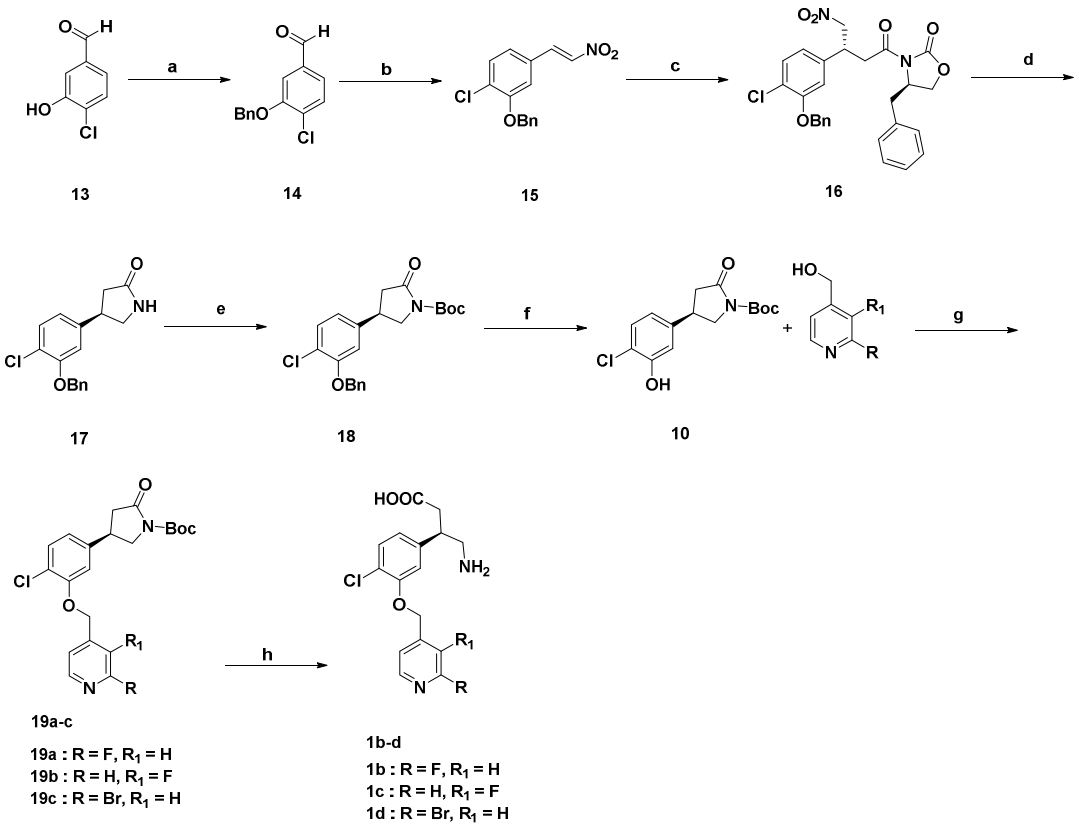

Reagents and conditions: a) Benzyl bromide, K_2CO_3, DMF, rt, 8h, 94%; b) Nitromethane, Ammonium acetate, Acetic acid, 105 °C to rt, 1.5h, 86%; c) **14**, NaHDMS, THF, -78 °C to rt, 2h, 53%; d) $NiCl_2 \cdot H_2O$,

$NaBH_4$, Ethanol, 0 °C to rt, 4h, 52%; e) Boc anhydride, DMAP, Et_3N, MC, 0 °C to rt, 8h, 90%; f) Pd/C, MeOH, rt, 0.5h, 80%; g) DIAD, PPh_3, THF, 0 °C to rt, 15h, 77%-84%; h) 1,4-Dioxane HCl at 90 °C for **1b** and 6N HCl at 90 °C for **1c** and concentrated HBr at 90 °C for **1d,** 12h, 37% to 73%.

***In vitro* assay**

The in vitro assay of compounds **1a-1c** and the reference compound, *R*-baclofen (*R*-**1**) was performed commercially (Eurofins-CEREP).

Functional agonist assay. The *in vitro* agonist activity assay at the human $GABA_B$ receptor expressed in transfected CHO cells[23] was performed by measuring an electric impedance modulation using the Cellular Dielectric Spectroscopy (CDS) detection method.[24]

Substitution of the aromatic ring of *R*-baclofen (*R*-**1**) with 4-pyridyl (**1a**)[4] or fluoro 4-pyridyl ether (**1b-1c**) resulted in a striking increase in the GABA-B % agonist response (Fig. **3**). The fluoro derivative **1b** exhibited the highest $GABA_B$ agonist response within the series **1a-1c**.

In vitro binding assay. In the $GABA_B$ radioligand binding assay studies, compound **1b** exhibited a greater binding inhibition than that of **1c** (34% and 15%, respectively, at concentration of 100 nM). Therefore, **1b** has been selected for further radiolabeling and animal experiments.

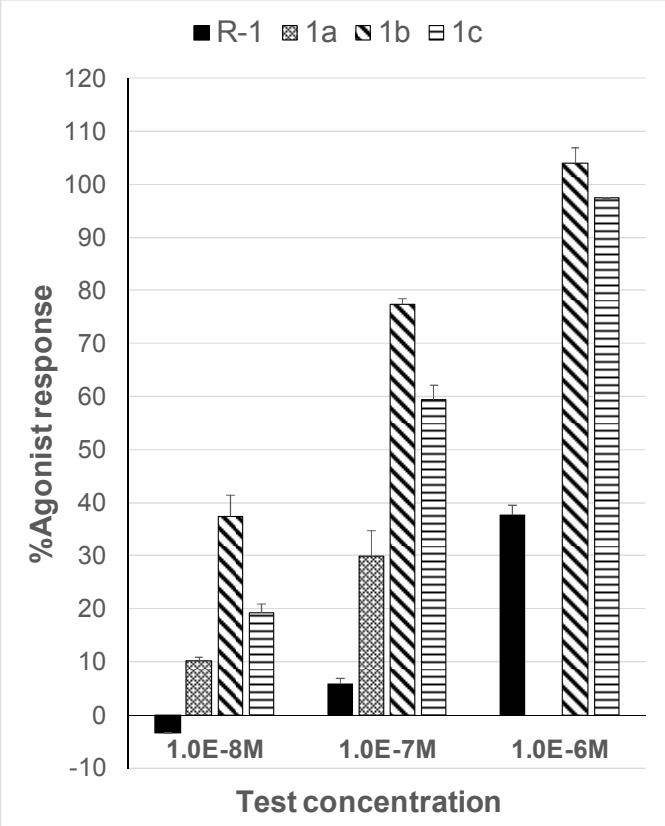

Figure 3. $GABA_B$ agonist effect of compounds **1a-1c** and *R*-baclofen (*R*-**1**) obtained by measuring an electric impedance modulation in the human $GABA_B$ receptor transfected CHO cells using the Cellular Dielectric Spectroscopy (CDS) detection method.

[a]Values are the means of % of control agonist response of two independent experiments, each in duplicate ± SD. Compound **1a** was not tested at the concentration of 10^{-6} M.

Radiochemistry

The radiolabeling of 2-fluoro-pyridine derivatives has been well established since the development of ^{18}F-derivatives of epibatidine.[25, 26] The labeling of **1b** with ^{18}F (code name [^{18}F]JHU11631) (Scheme **4**) was performed remotely in one step using a Kryptofix 222®, - assisted radiofluorination of the respective bromo-precursor **1d** in a modified MicroLab radiochemistry box (GE). The radiolabeling required high temperature (180°C) and DMSO was used as the reaction solvent. The synthesis was performed using mild base, $K_2C_2O_4$, under the conditions described previously.[27] The reaction was followed by a semi-

preparative HPLC separation using the general procedure.[25] The radiolabeled product [^{18}F]**1b** and precursor **1d** were fully separated by preparative HPLC (R_t = 15.5 and 23 min, respectively). Precursor was not detected by analytical HPLC in the final product solution.

The final product [^{18}F]**1b** was prepared with a radiochemical yield of 12-18% (n = 5, end of synthesis, non-decay-corrected), with a molar radioactivity in the range of 330–515 GBq/μmol (9–14 Ci/μmol) and a radiochemical purity greater than 97%. The final product [^{18}F]**1b** (72 - 86 mCi) was formulated as a solution in sterile saline containing 7% ethanol.

It is noteworthy that radiolabelling of [^{18}F]**1b** did not require a protection of liable -NH_2 and -COOH protons in the precursor molecule. This may be explained by a relatively large molecular fragment between the ^{18}F-atom and liable protons and in agreement with ^{18}F-labeling of other compounds with liable protons.[25]

Scheme 4. Radiosynthesis of [^{18}F]**1b**.

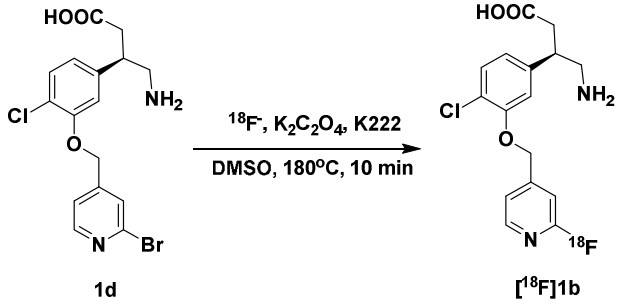

Biodistribution studies of [^{18}F]1b in mice

Baseline studies in CD-1 mice.

The regional brain distribution of the radiotracer [^{18}F]**1b** was studied in CD-1 male mice. The radioligand entered the mouse brain with peak (15 min) radioactivity accumulation of ~25%ID/g*body

weight (~ 1%ID/g tissue) followed by rapid washout (Table 1). The observed brain uptake is moderate and it is equal to the threshold uptake for selection of good PET tracer in our lab. The accumulation of radioactivity was seen in various subcortical and cortical regions including superior colliculus, striatum, hypothalamus, thalamus, cortex and cerebellum.

Previous *in vitro* autoradiography studies demonstrated that $GABA_B$ is widely distributed throughout the rodent brain regions.[28-30] The published *in vitro* data are not sufficient for defining a detailed regional brain distribution pattern, but the presence of $GABA_B$ was observed in the superior colliculus, thalamus and molecular layers of cerebellum.[28] The previous *in vitro* data agree with *in vivo* distribution of [^{18}F]**1b** in the CD-1 mouse brain (Table 1).

Table 1. Regional brain uptake of [^{18}F]**1b** at different time-points post iv injection. Abbreviators: CB–cerebellum; Hyp–hypothalamus; F. Ctx–frontal cortex; Ctx–cortex; Th–thalamus; Str–striatum; S. Coll–superior colliculus; REST–the rest of brain. Data: mean %ID/g tissue*body weight ± SD (n = 6).

Regions	15 min	SD	60 min	SD	120 min	SD	240 min	SD
Hyp	23.78	1.65	6.03	1.71	3.22	1.02	2.10	0.62
Str	24.66	3.29	4.23	0.65	2.31	0.58	1.74	0.48
F.Ctx	20.95	2.83	3.55	0.59	1.53	0.37	1.10	0.25
Ctx	20.64	3.25	3.16	0.53	1.27	0.29	0.88	0.22
Th	23.45	2.96	4.38	0.46	1.90	0.47	1.43	0.33
S.Coll	22.54	3.68	4.41	0.59	1.92	0.34	1.43	0.29
CB	21.51	2.92	4.62	0.84	1.61	0.28	1.09	0.19
REST	23.45	3.13	3.77	0.42	1.58	0.39	0.94	0.18

Specificity of [^{18}F]1b Binding in the Mouse Brain

A conventional *in vivo* blockade methodology was used for demonstration of the binding specificity of [^{18}F]**1b** radiotracer at the $GABA_B$ receptor in the mouse brain. A blockade study with a drug that is highly selective at the target binding site is expected to show the specificity of the radioligand binding. In the blocking experiment a pre-injection of **1a** (0.3 mg/kg, ip), a selective $GABA_B$ agonist[4], significantly reduced (~35%) the uptake of [^{18}F]**1b** in the whole brain of CD-1 mice. This study demonstrated that the binding of [^{18}F]**1b** is specific in the mouse brain and, at least, partially mediated by the $GABA_B$ receptors. Noteworthy, that at a higher dose of blocker (1 mg/kg) the tracer uptake increased (not shown). This is a common observation in the cases when the binding site is present in the periphery and injection of blocker increases the blood input function of radiotracers. Expression of $GABA_B$ in various peripheral organs is well documented.[31]

The demonstrated specific brain uptake of [^{18}F]**1b** in mice are below the conventional 50% threshold for a good PET tracer. Nevertheless, previous *in vitro* $GABA_B$ autoradiography showed a substantial species difference. There was greater $GABA_B$ density (B_{max}) in the non-human primates (50-437 fmol/mg tissue[32]) and human brain (60–700 fmol/mg tissue[33, 34]) than that in rodents (52 fmol/g tissue[27]). These numbers have to be used carefully because different research groups using different experimental protocols obtained them. Still, the species difference is encouraging and the greater $GABA_B$ levels in the primates may justify further PET studies with [^{18}F]**1b** and development of new $GABA_B$ PET tracers with improved $GABA_B$ binding affinity and BBB permeability.

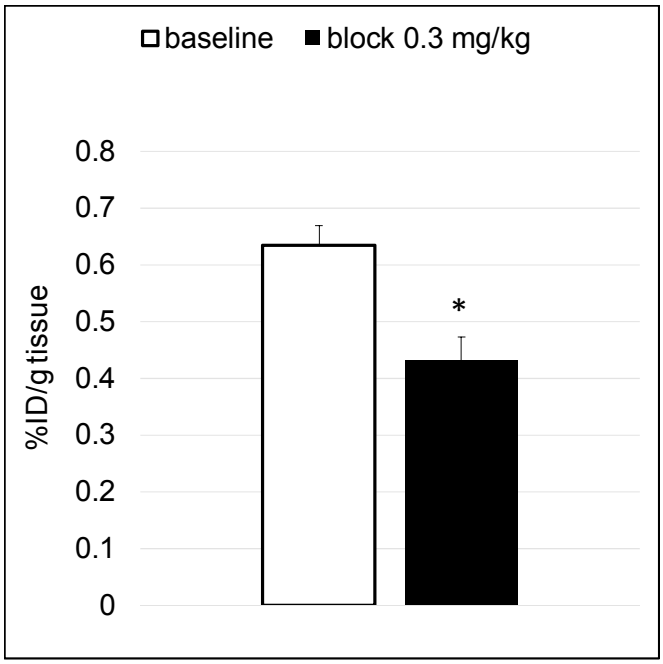

Figure 5. Blockade of [^{18}F]**1b** accumulation in the whole brain of CD1 mice by injection of the selective $GABA_B$ agonist **1a** (0.3 mg/kg, ip). Time point – 30 min post radiotracer injection. The data are the mean % injected dose/g tissue ± SD (n=5). The data show that administration of **1a** significantly reduces the whole brain uptake (*$P < 0.01$, ANOVA).

Experimental

All reagents were used directly as obtained commercially unless otherwise noted. Reaction progress was monitored by thin-layer chromatography (TLC) using silica gel 60 F254 (0.040−0.063 mm) with detection by UV. All moisture-sensitive reactions were performed under an argon atmosphere using oven-dried glassware and anhydrous solvents. Column flash chromatography was carried out using BDH silica gel 60Å (40−63 micron). Analytical TLC was performed on plastic sheets coated with silica gel 60 F254 (0.25 mm thickness, E. Merck, Darmstadt, Germany). ^{1}H and ^{13}C-NMR spectra were recorded with a Bruker-500 NMR spectrometer at nominal resonance frequencies of 500 MHz in $CDCl_3$, CD_3OD or

DMSO-d_6 (referenced to internal Me_4Si at δ 0 ppm). The chemical shifts (δ) were expressed in parts per million (ppm). High-resolution mass spectra were recorded utilizing electrospray ionization (ESI) at the University of Notre Dame Mass Spectrometry facility. All compounds that were tested in the biological assays were analysed by combustion analysis (CHN) to confirm a purity of >95%. A dose calibrator (Capintec 15R) was used for all radioactivity measurements. Radiolabeling was performed with a modified GE MicroLab radiochemistry module. HPLC purification and analysis of radiolabeled compounds were performed with Agilent 1260 Infinity System with UV detector and a Bioscan Flow-Count interface with a NaI radioactivity detector. The experimental animal protocols were approved by the Animal Care and Use Committee of the Johns Hopkins Medical Institutions.

Chemistry

(*R*)-4-(4-chlorophenyl)pyrrolidin-2-one (5): To *R*-baclofen (*R*-**1)** (1 g, 4.68 mmol) was added 10 mL of acetic acid. The reaction mixture was refluxed overnight. The mixture was cooled to room temperature, the acetic acid was removed *in vacuo* and the resultant mixture treated with water (100 mL). An off-white product precipitated and was filtered, washed with hexane and dried *in vacuo* to provide the (*R*)-4-(4-chlorophenyl)pyrrolidin-2-one as a white solid (0.9 g, 99.3% yield). ^{1}H NMR (500 MHz, CD_3OD) δ 7.33–7.22 (m, 4H), 3.79–3.64 (m, 2H), 3.39–3.32 (m, 1H), 2.73–2.66 (dd, J = 16.8, 8.8 Hz, 1H), 2.47–2.40 (dd, J = 16.8, 8.8 Hz, 1H).

(*R*)-4-(4-chloro-3-nitrophenyl)pyrrolidin-2-one (6): (*R*)-4-(4-chlorophenyl)pyrrolidin-2-one **5** (0.9 g, 4.6 mmol) was treated with sulfuric acid (5 mL). This solution was cooled in ice. Guanidine nitrate (0.56 g, 4.6 mmol) was added in portions. The reaction mixture was warmed to room temperature and stirred for 1 h. The mixture was then poured into ice water and extracted with ethyl acetate. The organic layer was separated, dried over anhydrous $MgSO_4$, filtered, and concentrated *in vacuo*. The resulting residue was purified by silica gel column chromatography (CH_2Cl_2: MeOH = 9:1) to give (*R*)-4-(4-chloro-3-

nitrophenyl)pyrrolidin-2-one as a yellow solid (1.05 g, 95.4% yield). ^{1}H NMR (500 MHz, $CDCl_3$) δ 7.77 (s, 1H), 7.55 (d, J = 10.0 Hz, 1H), 7.44 (d, J = 10.0 Hz, 1H), 6.13 (s, 1H), 3.86 (t, J = 10.0 Hz, 1H), 3.80–3.76 (m, 1H), 3.44–3.41 (m, 1H), 2.84–2.79 (m, 1H), 2.49–2.44 (m, 1H).

(*R*)-4-(3-amino-4-chlorophenyl)pyrrolidin-2-one (7): To a mixture of (*R*)-4-(4-chloro-3-nitrophenyl)pyrrolidin-2-one **6** (1.0 g, 4.15 mmol), and NH_4Cl (2.21 g, 41.5 mmol) in THF/MeOH/H_2O (10:5:3) (20 mL), was added Zn dust (2.71 g, 41.5 mmol) at 90 ˚C, then the mixture was refluxed for 1 h. After completion of the reaction, the reaction mixture was filtered through Celite and partitioned between EtOAc and brine. The organic layer was separated, dried over anhydrous $MgSO_4$, filtered, and concentrated *in vacuo*. The resulting residue was purified by silica gel column chromatography (CH_2Cl_2: MeOH = 9:1) to give (*R*)-4-(3-amino-4-chlorophenyl)pyrrolidin-2-one as a pale yellow solid (0.85 g, 97.1% yield). ^{1}H NMR (500 MHz, CD_3OD) δ 7.12–7.11 (d, J = 8.4 Hz, 1H), 6.74–6.73 (d, J = 2.0 Hz, 1H), 6.55–6.52 (m, 1H), 3.74–3.70 (m, 1H), 3.62–3.54 (m, 1H), 3.34–3.29 (m, 1H), 2.69–2.63 (dd, J = 16.4, 8.8 Hz,1H), 2.43–2.37 (dd, J = 16.4, 8.4 Hz, 1H).

(*R*)-4-(4-chloro-3-iodophenyl)pyrrolidin-2-one (8): To (*R*)-4-(3-amino-4-chlorophenyl)pyrrolidin-2-one **7** (0.8 g, 3.80 mmol) was added a mixture of 12N HCl (20 mL) and cooled to 0 °C. Sodium nitrite (0.29 g, 4.17 mmol) in 10 mL water was added dropwise. The mixture was stirred for 30 minutes. Potassium iodide (5.35 g, 32.3 mmol) in 50 mL of water was added dropwise at 0 °C. The mixture was stirred for 1h at 0 °C and then 45 minutes at room temperature. The reaction mixture was then partitioned between EtOAc and washed with 10% sodium thiosulfate, followed by water and brine. The organic layer was separated, dried over anhydrous $MgSO_4$, filtered, and concentrated *in vacuo*. The resulting residue was purified by silica gel column chromatography (CH_2Cl_2: MeOH = 9.5:0.5) to give (*R*)-4-(4-chloro-3-iodophenyl)pyrrolidin-2-one as a pale yellow solid (1.0 g, 82.0% yield). ^{1}H NMR (500 MHz, $CDCl_3$) δ 7.74 (s, 1H), 7.41 (d, J = 10.0 Hz, 1H), 7.19 (d, J = 10.0 Hz, 1H), 6.88 (s, 1H), 3.79 (t, J = 10.0 Hz, 1H), 3.64–3.61 (m, 1H), 3.40–3.36 (m, 1H), 2.77–2.71 (m, 1H), 2.46–2.41 (m, 1H).

***Tert*-butyl (*R*)-4-(4-chloro-3-iodophenyl)-2-oxopyrrolidine-1-carboxylate (9):** To the compound (*R*)-4-(4-chloro-3-iodophenyl)pyrrolidin-2-one **8** (1.0 g, 3.11 mmol) in CH_2Cl_2 (10 mL) was added DMAP (0.037 g, 0.031 mmol), triethylamine (0.37 g, 3.73 mmol) and di-*tert*-butyl dicarbonate (0.81 g, 3.73 mmol) at 0 °C, and then the mixture was stirred at room temperature for 12 h. After completion of the reaction it was diluted with CH_2Cl_2 and washed with brine, dried over anhydrous MgSO4, filtered, and concentrated *in vacuo*. Flash chromatography of the residue over silica gel (hexane:EtOAc = 9.5:0.5) afforded *tert*-butyl (*R*)-4-(4-chloro-3-iodophenyl)-2-oxopyrrolidine-1-carboxylate as a pale yellow solid (1.21 g, 92.3% yield). ^{1}H NMR (500 MHz, $CDCl_3$) δ 7.73 (s, 1H), 7.43 (d, J = 10.0 Hz, 1H), 7.17 (d, J = 10.0 Hz, 1H), 4.16–4.12 (m, 1H), 3.66–3.63 (m, 1H), 3.49–3.46 (m, 1H), 2.92–2.87 (m, 1H), 2.68–2.62 (m, 1H), 1.54 (s, 9H).

***Tert*-butyl (*R*)-4-(4-chloro-3-hydroxyphenyl)-2-oxopyrrolidine-1-carboxylate (10):** To a solution of *tert*-butyl (*R*)-4-(4-chloro-3-iodophenyl)-2-oxopyrrolidine-1-carboxylate **9** (1.2 g, 2.84 mmol) and Bis(pinacolato)diboron (2.16 g, 8.53 mmol) in DMF (12.0 mL) was added Pd(dppf)Cl_2.DCM (0.23 g, 0.028 mmol) and potassium acetate (1.11 g, 11.38 mmol). The reaction mixture was stirred at 90 °C for 12 h. After it cooled down to room temperature, to this solution, 35% hydrogen peroxide (12 mL) was added dropwise and stirred overnight at room temperature. The mixture was diluted with saturated ammonium chloride aqueous solution and extracted with dichloromethane (3 times). The combined organic layers were dried over Na_2SO_4 and concentrated under reduced pressure. The crude product was purified by column chromatography (Hexane/EtOAc = 3:7) to afford *tert*-butyl (*R*)-4-(4-chloro-3-hydroxyphenyl)-2-oxopyrrolidine-1-carboxylate as white solid (0.15 g, 17.0% yield). ^{1}H NMR (500 MHz, $CDCl_3$) δ 7.30 (d, J = 10.0 Hz, 1H), 6.91 (s, 1H), 6.75 (d, J = 10.0 Hz, 1H), 4.16–4.12 (m, 1H), 3.67–3.64 (m, 1H), 3.50–3.46 (m, 1H), 2.91–2.86 (m, 1H), 2.69–2.64 (m, 1H), 1.54 (s, 9H).

(*R*)-4-amino-3-(4-chloro-3-(pyridin-4-ylmethoxy)phenyl)butanoic acid (1a): To a solution of *tert*-butyl (*R*)-4-(4-chloro-3-hydroxyphenyl)-2-oxopyrrolidine-1-carboxylate **10** (0.1 g, 0.32 mmol) in ethanol (2 mL) was added K_2CO_3 (0.09 g, 0.64 mmol) followed by 4-(bromomethyl)pyridine hydrobromide

(0.121 g, 0.48 mmol). The reaction mixture was heated overnight at 90 °C. The mixture was cooled to room temperature and the solvent removed. The crude residue was treated with 6N HCl aqueous solution (4 mL) and heated for 3 h at 90 °C. After that reaction mixture was cooled and adjusted to pH to 7 by using aqueous $NaHCO_3$ solution. The precipitate was filtered, washed with cold water and dried to give (*R*)-4-amino-3-(4-chloro-3-(pyridin-4-ylmethoxy)phenyl)butanoic acid as a pale brown solid (0.07 g, 68.6% yield). ^{1}H NMR (500 MHz, CD_3OD) δ 8.91 (d, J = 10.0 Hz, 2H), 8.26 (d, J = 10.0 Hz, 2H), 7.45 (d, J = 10.0 Hz, 1H), 7.18 (s, 1H), 7.03 (d, J = 10.0 Hz, 1H), 5.60 (s, 2H), 3.83–3.75 (m, 2H), 3.44–3.41 (m, 1H), 2.77–2.72 (m, 1H), 2.52–2.47 (m, 1H). ^{13}C NMR (125 MHz, MeOD) δ 178.3, 158.6, 153.2, 143.4, 141.8, 130.3, 124.2, 121.2, 120.9, 112.6, 68.0, 49.2, 39.9, 37.7. HRMS (ESI+) *m/z* calcd $[C_{16}H_{18}ClN_2O_3]$ $[(M + H)]^+$ 321.1006, found 321.0987.

(*R*)-3-Acetyl-4-phenylmethyl-2-oxazolidinone (12): To a 250 mL round bottom flask equipped with a stir bar, 10 g (56.43 mmol) of (*R*)-4- phenylmethyl-2-oxazolidinone **11** was added, along with 100 mL of THF under N_2. The flask was then cooled to -78 °C, and 37.0 mL (59.30 mmol) of *n*-BuLi (1.6 M in hexanes) was added. After 20 minutes 4.1 mL (57.50 mmol) of acetyl chloride was added dropwise. After 30 minutes the reaction mixture was allowed to warm to room temperature and stirred for 3h. After that the reaction mixture was quenched with 100 mL of satd. aq. NH_4Cl. The majority of the THF was removed *in vacuo*. Methylene chloride was added and this solution was washed with 10% aq. NaOH. The aqueous layer was extracted again with CH_2Cl_2 (2 x 30 mL). The combined organic layers were washed with brine, dried with sodium sulfate, filtered, and concentrated *in vacuo* to yield (*R*)-3-Acetyl-4-phenylmethyl-2-oxazolidinone as a white solid (11.0 g, 88.9% yield). ^{1}H NMR (500 MHz, $CDCl_3$) δ 7.35–7.33 (m, 2H), 7.29 (d, J = 10.0 Hz, 1H), 7.21 (d, J = 10.0 Hz, 2H), 4.69–4.66 (m, 1H), 4.19 (t, J = 10.0, 2H), 3.33 (d, J = 10.0, 1H), 2.78 (d, J = 10.0, 1H), 2.56 (s, 3H). ^{13}C NMR (125 MHz, $CDCl_3$) δ 170.3, 153.7, 135.3, 129.4, 129.0, 127.4, 66.1, 55.0, 37.8, 23.8.

3-(Benzyloxy)-4-chlorobenzaldehyde (14): To a stirred solution of 4-chloro-3-hydroxybenzaldehyde **13** (5.0 g, 31.93 mmol) in DMF (40.0 mL) was added benzyl bromide (6.55 g, 38.3 mmol) and K_2CO_3 (22.05

g, 159.68 mmol). Then, the mixture was stirred at room temperature for 8h and then partitioned between EtOAc and brine. The organic layer was separated, washed with brine, dried over anhydrous MgSO4, filtered, and concentrated *in vacuo*. The resulting residue was purified by silica gel column chromatography (hexane:EtOAc = 1:9) to give 3-(benzyloxy)-4-chlorobenzaldehyde as a white solid (7.4 g, 93.9% yield). ^{1}H NMR (500 MHz, $CDCl_3$) δ 9.92 (s, 1H), 7.56 (d, J = 5.0 Hz, 2H), 7.50–7.47 (m, 3H), 7.42–7.39 (m, 3H), 7.35 (d, J = 10.0 Hz, 1H), 5.22 (s, 2H). ^{13}C NMR (125 MHz, $CDCl_3$) δ 190.9, 154.9, 136.0, 135.8, 130.9, 130.3, 128.7, 128.3, 127.2, 124.4, 111.9, 70.9.

(*E*)-2-(benzyloxy)-1-chloro-4-(2-nitrovinyl)benzene (15): 3-(benzyloxy)-4-chlorobenzaldehyde **14** (7.0 g, 28.37 mmol) was dissolved in acetic acid (8.5 mL), which was followed by the addition of nitromethane (35.0 mL) and ammonium acetate (5.46 g, 70.94 mmol). The resulting solution was heated to 105 °C for 90 minutes after which it was cooled and the solvent was evaporated under reduced pressure. The residue was triturated with water (100 mL), resulting in a yellow precipitate, which was filtered to obtain (*E*)-2-(benzyloxy)-1-chloro-4-(2-nitrovinyl)benzene as a yellow solid (7.1 g, 86.0% yield). ^{1}H NMR (500 MHz, $CDCl_3$) δ 7.92 (d, J = 15.0 Hz, 1H), 7.52–7.46 (m, 4H), 7.44–7.41 (m, 2H), 7.36 (d, J = 10.0 Hz, 1H), 7.11 (d, J = 10.0 Hz, 1H), 7.08 (d, J = 10.0 Hz, 1H), 5.21 (s, 2H). ^{13}C NMR (125 MHz, $CDCl_3$) δ 154.8, 138.1, 137.4, 131.3, 128.8, 128.7, 128.4, 127.3, 127.2, 127.1, 126.6, 113.7, 70.9.

(*R*)-4-benzyl-3-((*R*)-3-(3-(benzyloxy)-4-chlorophenyl)-4-nitrobutanoyl)oxazolidin-2-one (16): A solution of (*R*)-3-acetyl-4-benzyloxazolidin-2-one (5.39 g, 24.06 mmol) in THF (70 mL) was cooled under a nitrogen atmosphere to -78 ^{o}C and a solution of NaHMDS (1M in THF, 26.95 mL, 25.77 mmol) was added dropwise and stirred for 1h. A solution of nitroalkene **15** (7.0 g, 24.16 mmol) in THF (35 mL) was added dropwise to the reaction solution and the mixture was stirred for a further hour. After quenching with a saturated solution of ammonium chloride (100 mL), the mixture was extracted with ethyl acetate (3 × 75 mL). The combined organic layers were washed with brine (100 mL), dried (Na_2SO_4) and evaporated under reduced pressure. The resulting residue was purified by silica gel column

chromatography (hexane:EtOAc = 1:9) to give (*R*)-4-benzyl-3-((*R*)-3-(3-(benzyloxy)-4-chlorophenyl)-4-nitrobutanoyl)oxazolidin-2-one as a pale yellow solid (6.5 g, 52.8% yield). ^{1}H NMR (500 MHz, $CDCl_3$) δ 7.47 (d, J = 5.0 Hz, 2H), 7.40 (t, J = 5.0 Hz, 2H), 7.38–7.32 (m, 4H), 7.29 (d, J = 10.0 Hz, 1H), 7.17 (d, J = 10.0 Hz, 2H), 6.90 (s, 1H), 6.83 (d, J = 10.0 Hz, 1H), 5.16 (s, 2H), 4.70–4.66 (m, 1H), 4.61–4.55 (m, 2H), 4.15 (t, J = 5.0 Hz, 2H), 4.13–4.10 (m, 1H), 3.53–3.48 (m, 1H), 3.29–3.22 (m, 2H), 2.76–2.72 (m, 1H). ^{13}C NMR (125 MHz, $CDCl_3$) δ 169.8, 153.4, 138.4, 136.2, 134.9, 130.8, 129.4, 129.0, 18.6, 128.1, 127.3, 123.1, 120.5, 113.7, 79.3, 71.0, 66.5, 55.1, 39.3, 38.6, 37.8.

(*R*)-4-(3-(benzyloxy)-4-chlorophenyl)pyrrolidin-2-one (17): The oxazolidinone **16** (6 g, 11.78 mmol) was dissolved in ethanol (110 mL), cooled to 0 °C and nickel chloride hexahydrate (2.80 g, 11.78 mmol) was added, followed by the portionwise addition sodium borohydride (4.90 g, 129.67 mmol). The resulting black suspension was stirred for two hours at 0°C and then allowed to warm to room temperature over a further two hour period. Diluted hydrochloric acid solution (2 M, 30 mL) was added slowly to the mixture and the excess solvent was evaporated under reduced pressure. The black residue was dissolved with ethyl acetate (50 mL) and stirred with diluted hydrochloric acid solution (2 M, 30 mL) until a colorless solution was obtained. The aqueous phase was extracted with ethyl acetate (2 × 50 mL), and the combined organic layers were dried (Na_2SO_4) and evaporated under reduced pressure. The residue was purified by flash column chromatography (SiO_2, ethyl acetate/hexanes, 8/2 then ethyl acetate/methanol, 9/1) to obtain (*R*)-4-(3-(benzyloxy)-4-chlorophenyl)pyrrolidin-2-one as a colorless solid (1.85 g, 52.1% yield over two steps). ^{1}H NMR (500 MHz, $CDCl_3$) δ 7.47 (d, J = 5.0 Hz, 2H), 7.40 (t, J = 5.0 Hz, 2H), 7.34 (d, J = 10.0 Hz, 2H), 6.83 (s, 1H), 6.80 (d, J = 10.0 Hz, 1H), 5.76 (s, 1H), 5.16 (s, 2H), 3.75 (t, J = 5.0 Hz, 2H), 3.65–3.62 (m, 1H), 3.34–3.31 (m, 1H), 2.74–2.68 (m, 1H), 2.44–2.39 (m, 1H). ^{13}C NMR (125 MHz, $CDCl_3$) δ 177.6, 154.3, 142.2, 136.3, 130.5, 128.6, 128.1, 127.2, 122.0, 119.9, 112.8, 70.9, 49.4, 40.0, 37.9.

***Tert*-butyl (*R*)-4-(3-(benzyloxy)-4-chlorophenyl)-2-oxopyrrolidine-1-carboxylate (18):** To the compound (*R*)-4-(3-(benzyloxy)-4-chlorophenyl)pyrrolidin-2-one **17** (1.5 g, 4.97 mmol) in CH_2Cl_2 (10

mL) was added DMAP (0.60 g, 0.497 mmol), triethylamine (0.603 g, 5.96 mmol) and di-*tert*-butyl dicarbonate (1.30 g, 5.96 mmol) at 0 °C, and then, the mixture was stirred at room temperature for 8h. After completion of the reaction diluted with CH_2Cl_2 and washed with brine, dried over anhydrous MgSO4, filtered, and concentrated *in vacuo*. Flash chromatography of the residue over silica gel (hexane:EtOAc = 8:2) afforded *tert*-butyl (*R*)-4-(3-(benzyloxy)-4-chlorophenyl)-2-oxopyrrolidine-1-carboxylate as a colorless solid (1.8 g, 90.4% yield). ^{1}H NMR (500 MHz, $CDCl_3$) δ 7.46 (d, J = 5.0 Hz, 2H), 7.39 (t, J = 5.0 Hz, 2H), 7.36–7.31 (m, 2H), 6.81 (s, 1H), 6.78 (d, J = 10.0 Hz, 1H), 5.16 (s, 2H), 4.14–4.10 (m, 1H), 3.63–3.59 (m, 1H), 3.48–3.44 (m, 1H), 2.88–2.83 (m, 1H), 2.65–2.59 (m, 1H), 1.54 (s, 9H). ^{13}C NMR (125 MHz, $CDCl_3$) δ 172.6, 154.4, 149.8, 140.5, 136.2, 130.7, 128.7, 128.2, 127.2, 122.5, 119.8, 112.8, 83.3, 71.0, 52.9, 40.2, 36.2, 28.0.

***Tert*-butyl (*R*)-4-(4-chloro-3-hydroxyphenyl)-2-oxopyrrolidine-1-carboxylate (10):** The compound **18** (1.60 g, 3.98 mmol) was dissolved in methanol (16 mL). Palladium hydroxide (0.32 g) on activated charcoal (20 wt%) was added to the suspension, flushed and pressurized with hydrogen (50 psi) and stirred for 30 minutes at room temperature. The reaction mixture was filtered through a Celite pad, and the filtrate was concentrated under reduced pressure. The residue was purified by flash column chromatography (ethyl acetate/hexanes) to obtain *tert*-butyl (*R*)-4-(4-chloro-3-hydroxyphenyl)-2-oxopyrrolidine-1-carboxylate as a colorless solid (1.0 g, 80.0% yield). ^{1}H NMR (500 MHz, $CDCl_3$) δ 7.30 (d, J = 10.0 Hz, 1H), 6.91 (s, 1H), 6.75 (d, J = 10.0 Hz, 1H), 4.16–4.12 (m, 1H), 3.67–3.64 (m, 1H), 3.50–3.46 (m, 1H), 2.91–2.86 (m, 1H), 2.69–2.64 (m, 1H), 1.54 (s, 9H). ^{13}C NMR (125 MHz, $CDCl_3$) δ 172.7, 151.7, 149.8, 141.4, 129.5, 119.6, 118.9, 114.7, 83.3, 52.8, 40.1, 35.9, 28.0.

***Tert*-butyl (*R*)-4-(4-chloro-3-((2-fluoropyridin-4-yl)methoxy)phenyl)-2-oxopyrrolidine-1-carboxylate (19a):** To a mixture of *tert*-butyl (*R*)-4-(4-chloro-3-hydroxyphenyl)-2-oxopyrrolidine-1-carboxylate **10** (0.2 g, 0.64 mmol) and PPh_3 (0.25 g, 0.96 mmol) in THF (10 mL) at 0 °C was added DIAD (0.196 g, 0.96 mmol). After stirring for 1 h, (2-fluoropyridin-4-yl)methanol (0.085 g, 0.67 mmol) was added to the reaction mixture 0 °C. The reaction mixture was stirred for 2 h at 0 °C and overnight at room temperature.

The resulting mixture was partitioned between ethyl acetate and water. The aqueous layer was extracted with ethyl acetate and the combined organic layers were dried (Na_2SO_4) and evaporated under reduced pressure. The residue was purified by flash column chromatography (ethyl acetate/hexanes) to obtain *tert*-butyl (*R*)-4-(4-chloro-3-((2-fluoropyridin-4-yl)methoxy)phenyl)-2-oxopyrrolidine-1-carboxylate as a colorless solid (0.2 g, 76.9% yield). ^{1}H NMR (500 MHz, $CDCl_3$) δ 8.28 (d, J = 5.0 Hz, 1H), 7.43 (d, J = 10.0 Hz, 1H), 7.32 (d, J = 5.0 Hz, 1H), 7.13 (s, 1H), 6.91 (s, 1H), 6.88 (d, J = 5.0 Hz, 1H), 6.80 (s, 1H), 5.20 (s, 2H), 4.19–4.15 (m, 1H), 3.69–3.65 (m, 1H), 3.53–3.50 (m, 1H), 2.95–2.90 (m, 1H), 2.71–2.65 (m, 1H), 1.56 (s, 9H). ^{13}C NMR (125 MHz, $CDCl_3$) δ 172.3, 153.7, 149.8, 148.1, 148.0, 141.0, 131.1, 122.6, 120.7, 118.8, 112.4, 107.3, 106.9, 83.4, 68.6, 52.9, 40.2, 36.1, 28.0.

***Tert*-butyl (*R*)-4-(4-chloro-3-((3-fluoropyridin-4-yl)methoxy)phenyl)-2-oxopyrrolidine-1-carboxylate (19b):** To a mixture of *tert*-butyl (*R*)-4-(4-chloro-3-hydroxyphenyl)-2-oxopyrrolidine-1-carboxylate **10** (0.2 g, 0.64 mmol) and PPh_3 (0.25 g, 0.96 mmol) in THF (10 mL) at 0 °C was added DIAD (0.196 g, 0.96 mmol). After stirring for 1 h, (3-fluoropyridin-4-yl)methanol (0.085 g, 0.67 mmol) was added to the reaction mixture 0 °C. The reaction mixture was stirred for 2 h at 0 °C and overnight at room temperature. The resulting mixture was partitioned between ethyl acetate and water. The aqueous layer was extracted with ethyl acetate and the combined organic layers were dried (Na_2SO_4) and evaporated under reduced pressure. The residue was purified by flash column chromatography (ethyl acetate/hexanes) to obtain *tert*-butyl (*R*)-4-(4-chloro-3-((3-fluoropyridin-4-yl)methoxy)phenyl)-2-oxopyrrolidine-1-carboxylate as a colorless solid (0.2 g, 76.9% yield). ^{1}H NMR (500 MHz, $CDCl_3$) δ 8.55 (s, 2H), 7.78 (s, 1H), 7.43 (d, J = 5.0 Hz, 1H), 6.91 (s, 1H), 6.88 (d, J = 5.0 Hz, 1H), 5.29 (s, 2H), 4.20–4.16 (m, 1H), 3.70–3.66 (m, 1H), 3.55–3.52 (m, 1H), 2.96–2.91 (m, 1H), 2.72–2.68 (m, 1H), 1.56 (s, 9H). ^{13}C NMR (125 MHz, $CDCl_3$) δ 172.3, 157.6, 153.6, 149.8, 144.3, 141.1, 131.1, 131.0, 123.4, 122.6, 120.9, 119.7, 112.6, 83.4, 63.4, 52.8, 40.3, 36.2, 28.1.

***Tert*-butyl (*R*)-4-(3-((2-bromopyridin-4-yl)methoxy)-4-chlorophenyl)-2-oxopyrrolidine-1-carboxylate (19c):** To a mixture of *tert*-butyl (*R*)-4-(4-chloro-3-hydroxyphenyl)-2-oxopyrrolidine-1-

carboxylate **10** (0.2 g, 0.64 mmol) and PPh_3 (0.25 g, 0.96 mmol) in THF (10 mL) at 0 °C was added DIAD (0.196 g, 0.96 mmol). After stirring for 1 h, (2-bromopyridin-4-yl)methanol (0.126 g, 0.67 mmol) was added to the reaction mixture 0 °C. The reaction mixture was stirred for 2 h at 0 °C and overnight at room temperature. The resulting mixture was partitioned between ethyl acetate and water. The aqueous layer was extracted with ethyl acetate and the combined organic layers were dried (Na_2SO_4) and evaporated under reduced pressure. The residue was purified by flash column chromatography (ethyl acetate/hexanes) to obtain *tert*-butyl (*R*)-4-(3-((2-bromopyridin-4-yl)methoxy)-4-chlorophenyl)-2-oxopyrrolidine-1-carboxylate as a colorless solid (0.26 g, 84.1% yield). ^{1}H NMR (500 MHz, $CDCl_3$) δ 8.43 (d, J = 5.0 Hz, 1H), 7.66 (s, 1H), 7.44–7.40 (m, 2H), 6.90 (d, J = 5.0 Hz, 1H), 6.79 (s, 1H), 5.15 (s, 2H), 4.19–4.15 (m, 1H), 3.69–3.65 (m, 1H), 3.53–3.50 (m, 1H), 2.95–2.90 (m, 1H), 2.71–2.65 (m, 1H), 1.56 (s, 9H). ^{13}C NMR (125 MHz, $CDCl_3$) δ 172.4, 153.7, 150.4, 149.7, 148.4, 142.7, 141.0, 131.0, 125.5, 122.5, 120.7, 120.3, 112.6, 83.3, 68.4, 52.9, 40.2, 36.2, 28.0.

(*R*)-4-amino-3-(4-chloro-3-((2-fluoropyridin-4-yl)methoxy)phenyl)butanoic acid (1b): To *tert*-butyl (*R*)-4-(4-chloro-3-((2-fluoropyridin-4-yl)methoxy)phenyl)-2-oxopyrrolidine-1-carboxylate **19a** (0.1 g, 2.37 mmol) was added 3 mL of HCl in 1,4-dioxane. The reaction mixture was refluxed overnight. The mixture was cooled to room temperature and adjusted to pH 7 by using aqueous $NaHCO_3$ solution. The precipitate was filtered, washed with cold water and dried to give (*R*)-4-amino-3-(4-chloro-3-((2-fluoropyridin-4-yl)methoxy)phenyl)butanoic acid as a white solid (0.03 g, 37.5% yield). ^{1}H NMR (500 MHz, $CDCl_3$) δ 8.26 (d, J = 10.0 Hz, 1H), 7.81(s, 1H), 7.59–7.56 (m, 1H), 7.46–7.40 (m, 2H), 7.30 (d, J = 10.0 Hz, 1H), 7.22 (d, J = 10.0 Hz, 1H), 7.11–7.06 (m, 1H), 4.68 (s, 1H), 3.64 (d, J = 10.0 Hz, 1H), 1.43–1.40 (m, 1H), 3.28 (d, J = 5.0 Hz, 1H), 2.32–2.29 (m, 1H), 1.84–1.82 (m, 1H), 1.76–1.73 (m, 2H), 1.72 (s, 9H), 1.60 (s, 1H), 1.54–1.47 (m, 1H), 1.43–1.37 (m, 1H), 1.28 (s, 3H), 1.15 (s, 3H), 1.09 (d, J = 10.0 Hz, 3H). ^{13}C NMR (125 MHz, MeOD) δ 178.4, 165.0, 153.6, 147.3, 147.2, 143.1, 130.2, 121.2, 120.3, 119.3, 112.6, 106.9, 68.0, 49.2, 39.9, 37.7. HRMS (ESI+) *m/z* calcd $[C_{16}H_{17}ClFN_2O_3]$ $[(M + H)]^+$ 339.0912, found 339.0906.

(*R*)-4-amino-3-(4-chloro-3-((3-fluoropyridin-4-yl)methoxy)phenyl)butanoic acid (1c): To *tert*-butyl (*R*)-4-(4-chloro-3-((3-fluoropyridin-4-yl)methoxy)phenyl)-2-oxopyrrolidine-1-carboxylate **19b** (0.1 g, 2.37 mmol) was added 3 mL of 6N HCl solution. The reaction mixture was refluxed overnight. The mixture was cooled to room temperature and adjusts the pH to 7 by using aqueous $NaHCO_3$ solution. The precipitate was filtered, washed with cold water and dried to give (*R*)-4-amino-3-(4-chloro-3-((3-fluoropyridin-4-yl)methoxy)phenyl)butanoic acid as a white solid (0.03 g, 37.5% yield). ^{1}H NMR (500 MHz, $CDCl_3$) δ 8.26 (d, J = 10.0 Hz, 1H), 7.81(s, 1H), 7.59–7.56 (m, 1H), 7.46–7.40 (m, 2H), 7.30 (d, J = 10.0 Hz, 1H), 7.22 (d, J = 10.0 Hz, 1H), 7.11–7.06 (m, 1H), 4.68 (s, 1H), 3.64 (d, J = 10.0 Hz, 1H), 1.43–1.40 (m, 1H), 3.28 (d, J = 5.0 Hz, 1H), 2.32–2.29 (m, 1H), 1.84–1.82 (m, 1H), 1.76–1.73 (m, 2H), 1.72 (s, 9H), 1.60 (s, 1H), 1.54–1.47 (m, 1H), 1.43–1.37 (m, 1H), 1.28 (s, 3H), 1.15 (s, 3H), 1.09 (d, J = 10.0 Hz, 3H). ^{13}C NMR (125 MHz, MeOD) δ 178.4, 153.6, 145.4, 143.2, 137.0, 136.8, 134.0, 130.2, 123.3, 121.3, 120.4, 112.7, 63.1, 49.2, 39.9, 37.7. HRMS (ESI+) *m/z* calcd $[C_{16}H_{17}ClFN_2O_3]$ $[(M + H)]^+$ 339.0912, found 339.0906.

(*R*)-4-amino-3-(4-chloro-3-((2-bromopyridin-4-yl)methoxy)phenyl)butanoic acid (1d): To *tert*-butyl (*R*)-4-(4-chloro-3-((2-bromopyridin-4-yl)methoxy)phenyl)-2-oxopyrrolidine-1-carboxylate **19c** (0.2 g, 0.415 mmol) was added 4 mL of 55% HBr solution. The reaction mixture was refluxed overnight. The mixture was cooled to room temperature and adjusted to pH 7 by using aqueous $NaHCO_3$ solution. The precipitate was filtered, washed with cold water and dried to give (*R*)-4-amino-3-(4-chloro-3-((3-bromopyridin-4-yl)methoxy)phenyl)butanoic acid as a white solid (0.12 g, 72.7% yield). ^{1}H NMR (500 MHz, $CDCl_3$) δ 8.26 (d, J = 10.0 Hz, 1H), 7.81(s, 1H), 7.59–7.56 (m, 1H), 7.46–7.40 (m, 2H), 7.30 (d, J = 10.0 Hz, 1H), 7.22 (d, J = 10.0 Hz, 1H), 7.11–7.06 (m, 1H), 4.68 (s, 1H), 3.64 (d, J = 10.0 Hz, 1H), 1.43–1.40 (m, 1H), 3.28 (d, J = 5.0 Hz, 1H), 2.32–2.29 (m, 1H), 1.84–1.82 (m, 1H), 1.76–1.73 (m, 2H), 1.72 (s, 9H), 1.60 (s, 1H), 1.54–1.47 (m, 1H), 1.43–1.37 (m, 1H), 1.28 (s, 3H), 1.15 (s, 3H), 1.09 (d, J = 10.0 Hz, 3H). ^{13}C NMR (125 MHz, MeOD) δ 178.4, 153.6, 150.3, 149.8, 143.1, 141.6, 130.2, 125.6,

121.2, 120.8, 120.4, 112.6, 67.7, 49.2, 39.9, 37.7. HRMS (ESI+) *m/z* calcd $[C_{16}H_{17}BrClN_2O_3]$ $[(M + H)]^+$ 399.0111, found 399.0106.

***In vitro* GABA$_B$ assay**

The in vitro assay of compounds **1a-1c** and R-baclofen (*R*-**1**) was performed commercially by Eurofins-CEREP.

GABA-B agonist assay. In brief, the human $GABA_B$ receptor transfected CHO cells were seeded onto a 96-well plate at a density of 8.10^4 cells/well in HBSS buffer + 20 mM HEPES and 0.1% BSA and were allowed to equilibrate for 60 min at 28°C before the start of the experiment. The assay was done in duplicate in two independent experiments. The system measured changes in electric impedance that occur in each well upon stimulation of cell surface receptors. Plates were placed onto the system and measurements are made at a temperature of 28 °C. Solutions are added simultaneously to all 96 wells using an integrated fluidics system: HBSS (basal control), reference agonist at 100 µM (stimulated control), reference agonist (EC_{50} determination) or the test compounds. Impedance measurements are monitored for 10 minutes after ligand addition. The standard reference agonist is 3-APMPA, which was tested in each experiment at several concentrations to generate a concentration-response curve from which its EC_{50} value is calculated.

GABA-B radioligand binding assay (Eurofins catalog number 228510). Source: Wistar Rat brain. Radiotracer: [^{3}H]CGP-54626, concentration 0.60 nM, Kd = 2.3 nM, B_{max} = 1.1 pmole/mg protein. Vehicle: 1% aq. DMSO. Non-specific ligand: CGP-54626, concentration 100 µM. Incubation conditions: 20 min at 25^{o}C. Incubation buffer: 50 mM Tris-HCl, pH 7.4, 2.5 mM $CaCl_2$. The assay was done in duplicate in two independent experiments at the concentration of test compound of 100 nM. Mean % inhibition was calculated.

Radiosynthesis of [^{18}F]1b.

A solution of the [^{18}F]fluoride prepared with a PETTrace cyclotron (General Electric; GE), 10 mg of Kryptofix 222®, and 1.6 mg of $K_2C_2O_4$ in 1 mL of 50% aqueous acetonitrile was added to a reaction vessel of a GE MicroLab module (Milwaukee, WI). The mixture was heated at 120-135 °C under a stream of argon, while water was evaporated azeotropically after the additions of 2 mL of CH_3CN. A solution of the corresponding bromo precursor **1d** (2 mg) in anhydrous DMSO (0.8 mL) was added to the reaction vessel and heated at 180 °C for 10 min. The reaction mixture was cooled, diluted with 0.7 mL of water and injected onto the reverse-phase semi-preparative HPLC: column Luna C18 10x250 mm, 10 micron (Phenomenex); mobile phase 32% acetonitrile: 68% 0.1M aqueous ammonium formate, 10 ml/min. The radioactive peak with a retention time of 15.5 min was collected in 50 mL of water. The aqueous solution was transferred through an activated Waters C-18 Sep-Pak Plus (Milford, MA) solid-phase extraction (SPE) cartridge. After washing the SPE with 10 mL saline, the product was eluted with a 1 mL of ethanol into a collection vial and 10 mL of 0.9% saline was added through the same SPE. The final product [^{18}F]**1b** was then analyzed by analytical HPLC using a UV detector at 254 nm to determine the radiochemical purity and molar radioactivity at the time the synthesis ended. The total synthesis time including QC was 65 min.

Analytical HPLC conditions: XBridge, 10 micron, 4.6 x 250 mm; mobile phase: 40:60 (acetonitrile: 0.1M aqueous ammonium formate); flow rate 3 mL/min; UV - 254 nm; retention time 3.1 min.

Biodistribution studies of [^{18}F]1b in CD-1 mice

Baseline study: Male, CD-1 mice weighing 25-30 g from Charles River Laboratories, (Wilmington, MA) were used for biodistribution studies. The animals were sacrificed by cervical dislocation at various times following injection of [^{18}F]**1b** (100 μCi, molar radioactivity 7200 mCi/μmol, in 0.2 mL saline) into a lateral tail vein; six animals per time point. The brains were rapidly removed and dissected on ice. The brain regions of interest were weighed and their radioactivity content was determined in an automated γ-counter with a counting error below 3%. Aliquots of the injectate were prepared as standards and their

radioactivity content was counted along with the tissue samples; the percent of injected dose per gram of tissue (%ID/g tissue) was calculated. All experimental protocols were approved by the Animal Care and Use Committee of the Johns Hopkins Medical Institutions.

***Blocking study**: In vivo* $GABA_B$ receptor blocking studies were carried out in CD-1 male mice (5 per group) by intraperitoneal (i.p.) administration of $GABA_B$ agonist **1a** (0.3 mg/kg) followed by i.v. injection of the radiotracer [^{18}F]**1b** (100 μCi, molar radioactivity ~6400 mCi/μmol, 0.1 mL, saline solution at pH = 5) 15 min thereafter. Control animals were injected with 0.1 mL of saline at pH = 5. Thirty min after the administration of **[^{18}F]1b** brain tissues were harvested, and their radioactivity content was determined.

Conclusion

In this study we synthesized $GABA_B$ agonists **1b-c** for PET imaging of $GABA_B$ in animals. The most potent agonist with greatest inhibition binding affinity **1b** was radiolabeled with ^{18}F with good radiochemical yield, high radiochemical purity and high molar radioactivity. The mouse experiments with the PET radiotracer [^{18}F]**1b** demonstrated the feasibility of *ex vivo* quantification of $GABA_B$ receptors. The future research on $GABA_B$ PET imaging should target radiotracers with improved specific binding and greater blood-brain barrier permeability.

AUTHOR INFORMATION

Corresponding Author

*Phone: (1) 410-614-5130; e-mail: ahorti1@jhmi.edu.

Author Contributions

Ravi Naik has synthesized all unlabeled compounds.

Andrew G. Horti and Dean F. Wong designed the experiments.

Andrew G. Horti and Dean F. Wong analyzed the animal data.

Andrew G. Horti and Ravi Naik were involved in writing the manuscript.

Andrew G. Horti and Robert F. Dannals were involved in radiosynthesis of $GABA_B$ radiotracer.

Heather Valentine, Andrew G. Horti, Ravi Naik were involved in the mouse studies.

Conflict of interest

The authors declare no competing financial interest.

Acknowledgements

This research was supported in part by SFARI (Simon Foundation Autism Research Initiative) grant (Wong, Horti) and Division of Nuclear Medicine and Molecular Imaging. We thank Paige Finley for the help with animal experiments and Julia Buchanan for editorial comments.

We thank Dr. Thomas Morley of Invicro (Boston, MA) for useful synthetic procedures related to the synthesis of compound **17**.

REFERENCES

(1) Kerr, D. I., and Ong, J. (1995) $GABA_B$ receptors. *Pharmacol*. *Ther*. 67, 187–246.

(2) Pinard, A., Seddik R., and Bettler, B. (2010) $GABA_B$ receptors: physiological functions and mechanisms of diversity. *Adv*. *Pharmacol*. *58*, 231–255.

(3) Bettler, B., Kaupmann, K., Mosbacher, J., and Gassmann, M. (2004) Molecular structure and physiological functions of $GABA_B$ receptors. *Physiol*. *Rev*. *84*, 835–867.

(4) Xu, F., Peng, G., Phan, T., Dilip, U., Chen, J. L., Chernov-Rogan, T., Zhang, X., Grindstaff, K., Annamalai, T., Koller, K., Gallop, M. A., and Wustrow, D. J. (2011) Discovery of a novel potent GABAB receptor agonist. *Bioorg*. *Med*. *Chem*. *Lett*. *21*, 6582–6585.

(5) Brennan, J. L., Leung, J. G., Gagliardi, J. P., Rivelli, S. K., and Muzyk, A.J. (2013) Clinical e□ectiveness of baclofen for the treatment of alcohol dependence: a review. *Clin*. *Pharmacol*. *5*, 99–107.

(6) Brusberg, M., Ravnefjord, A., Martinsson, R., Larsson, H., Martinez, V., and Lindström, E. (2009) The GABA receptor agonist, baclofen, and the positive allosteric modulator, CGP7930, inhibit visceral pain-related responses to colorectal distension in rats. *Neuropharmacology 56*, 362–367.

(7) Wahlstrom-Helgren, S., and Klyachko, V. A. (2015) Neuroscience $GABA_B$ receptor-mediated feed-forward circuit dysfunction in the mouse model of fragile X syndrome. *J*. *Physiol. 593*(22), 5009–5024.

(8) Serge, P. (2011) Medicaments for the prevention and treatment of a disease associated with retinal ganglion cell degeneration. *Patent applications*. WO 2011113904 A1.

(9) Collins, A. L., Ma, D., Whitehead, P. L., Martin, E. R., Wright, H. H., Abramson, R. K., Hussman, J. P., Haines, J. L., Cuccaro, M. L., Gilbert, J. R., and Pericak-Vance, M. A. (2006) Investigation of autism and GABA receptor subunit genes in multiple ethnic groups. *Neurogenetics 7*, 167–174.

(10) Xu, F., Gallop, M. A., Peng, G., Phan, T., Dilip, U., and Wustrow, D. J. (2010) Gamma-amino-butyric acid derivatives as gabab receptor ligands. *Patent application*, WO 2010/120370 A2.

(11) Diagnostic and statistical manual of mental disorders: 4th ed. Washington (DC): American Psychiatric Association; 1994 [cited 2010 Mar 8]. 866 p.

(12) Baird, G., Simonoff, E., Pickles, A., Chandler, S., Loucas, T., Meldrum, D., and Charman, T. (2006) Prevalence of disorders of the autism spectrum in a population cohort of children in South Thames: the Special Needs and Autism Project (SNAP). *Lancet 368*, 210–215.

(13) Levy, S. E., Mandell, D. S. and Schultz,R. T. (2009) Autism. *Lancet*, *374*, 1627–1638.

(14) Silverman, J. L., Pride, M. C., Hayes, J. E., Puhger, K. R., Butler-Struben, H. M., Baker, S., and Crawley,J. N. (2015) $GABA_B$ Receptor Agonist R-Baclofen Reverses Social Deficits and Reduces Repetitive Behavior in Two Mouse Models of Autism. *Neuropsychopharmacology 40*, 2228–2239.

(15) Fatemi, S. H., Folsom, T. D., Reutiman, T. J., and Thuras, P. D. (2009) Expression of $GABA_B$ Receptors Is Altered in Brains of Subjects with Autism. *Cerebellum 8*, 64–69.

(16) Kato, K., Zhang, M. R., and Suzuki, K. (2009) Synthesis of (*R*,*S*)-[4-^{11}C]baclofen via Michael addition of nitromethane labeled with short-lived ^{11}C. *Bioorg*. *Med*. *Chem*. *Lett*. *19*, 6222–6224.

(17) Todde, S., Moresco, R. M., Frostl, W., Stampf, P., Matarrese, M., Carpinelli, A., Magni, F., Galli Kienle, M., and Fazio, F. (2000) Synthesis and *in vivo* evaluation of [^{11}C]CGP62349, a new $GABA_B$ receptor antagonist. *Nucl*. *Med*. *Biol*. *27*, 565–569.

(18) Moran, M. D., Wilson, A. A., Elmore, C. S., Parkes, J., Ng, A., Sadovski, O., Graff, A., Daskalakis, Z. Houle, J., S., Chapdelaine, M. J., and Vasdev, N. (2012) Development of new carbon-11 labelled radiotracers for imaging $GABA_A$- and $GABA_B$-benzodiazepine receptors. *Bioorg*. *Med*. *Chem*. *20*, 4482–4488.

(19) Sambasivarao, K., Kakali, L., and Dhurke, K. (2002) Recent applications of the Suzuki–Miyaura cross-coupling reaction in organic synthesis. *Tetrahedron 58*, 9633–9695.

(20) Thomae, D., Morley, T. J., Lee, H. S., Barret, O., Constantinescu, C., Papin, C., Baldwin, R. M., Tamagnan, G. D., and Alagille, D. (2016) Identification and *in vivo* evaluation of a fluorine-18

rolipram analogue, [^{18}F]MNI-617, as a radioligand for PDE4 imaging in mammalian brain. *J. Label. Compd. Radiopharm.* *59*, 205–213.

(21) Lloyd, D. H., and Nichols, D. E. (1986) Nickel boride/hydrazine hydrate reduction of aromatic and aliphatic nitro compounds. Synthesis of 4-(benzyloxy)indole and .alpha.-alkyltryptamines. *J. Org. Chem.* *51*, 4294–4295.

(22) Kumara Swamy, K. C., Bhuvan Kumar, N. N., Balaraman, E., and Pavan Kumar, K. V. P. (2009) Mitsunobu and Related Reactions: Advances and Applications. *Chem. Rev.* *109*, 2551–2651.

(23) Hirst,W. D., Babbs, A. J., Green, A., Minton, J. A., Shaw, T. E., Wise, A., Rice, S. Q., Pangalos, M. N., and Price, G. W. (2003) Pharmacological characterisation of a cell line expressing $GABA_{B1b}$ and $GABA_{B2}$ receptor subunits. *Biochem. Pharmacol.* *65*, 1103–1113.

(24) Ciambrone, G. J., Liu, V. F., Lin, D. C., McGuinness, R. P., Leung, G. K., and Pitchford, S. (2004) Cellular Dielectric Spectroscopy: A Powerful New Approach to Label-Free Cellular Analysis. *J. Biomol. Screen.* *9*(6), 467–480.

(25) Horti, A., Ravert, H. T., London, E. D., and Dannals, R. F. (1996) Synthesis of a radiotracer for studying nicotinic acetylcholine receptors: (+/−)-exo-2-(2-[^{18}F]fluoro-5-pyridyl)-7-azabicyclo[2.2.1]heptane. *J. Label. Compd. Radiopharm.*, 1996, *38*, 355–365.

(26) Dolle, F. (2005) Fluorine-18-labelled fluoropyridines: advances in radiopharmaceutical design. *Curr. Pharm. Des.* *11*, 3221–3235.

(27) Ross, T. L., and Ametamey, S. M. (2011) PET Radiochemistry: An Introduction, p.75. In Basic Sciences of Nuclear Medicine, Ed. By M.M.Khalil, Springer. ISBN 978-3-540-85961-1.

(28) Bowery, N. G., Hudson, A. L., and Price, G. W. (1987) $GABA_A$ and $GABA_B$ receptor site distribution in the rat central nervous system. *Neuroscience 20*, 365–383.

(29) Chu, D. C. M., Albin, R. L., Young, A. B. and Penney, J. B. (1990) Distribution and kinetics of $GABA_B$ binding sites in rat central nervous system: A quantitative autoradiographic study. *Neuroscience 34*, 341–357.

(30) Mathew, J., Balakrishnan, S., Antony, S., Abraham, P. M., and Paulose, C. S.(2012) Decreased GABA receptor in the cerebral cortex of epileptic rats: effect of *Bacopa monnieri* and Bacoside-A. *J. Biomed. Sci. 19*, 19–25.

(31) Castelli, M. P., Ingianni, A., Stefanini, E., and Gessa, G. L. (1999) Distribution of $GABA_B$ receptor mRNAs in the rat brain and peripheral organs. *Life Sci. 64*(15), 1321–1328.

(32) Ambardekar, A. V., Ilinsky, I. A., Forestl, W., Bowery, N. G., and Kultas-Ilinsky, K. (1999) Distribution and properties of $GABA_B$ antagonist [^{3}H]CGP 62349 binding in the rhesus monkey thalamus and basal ganglia and the influence of lesions in the reticular thalamic nucleus. *Neuroscience 93*, 1339–1347.

(33) Billinton, A., Baird, V. H., Thom, M., Duncan, J. S., Upton, N., and Bowery, N. G. (2001) $GABA_B$ receptor autoradiography in hippocampal sclerosis associated with human temporal lobe epilepsy. *Br. J. Pharmaco*l. *132*, 475–480.

(34) Princivalle, A. P., Duncan, J. S., Thom, M., and Bowery, N. G. (2002) Studies of GABAB receptors labelled with [3H]-CGP62349 in hippocampus resected from patients with temporal lobe epilepsy. *Br. J. Pharmacol*., 2002, 136, 1099–1106.

Table of Contents

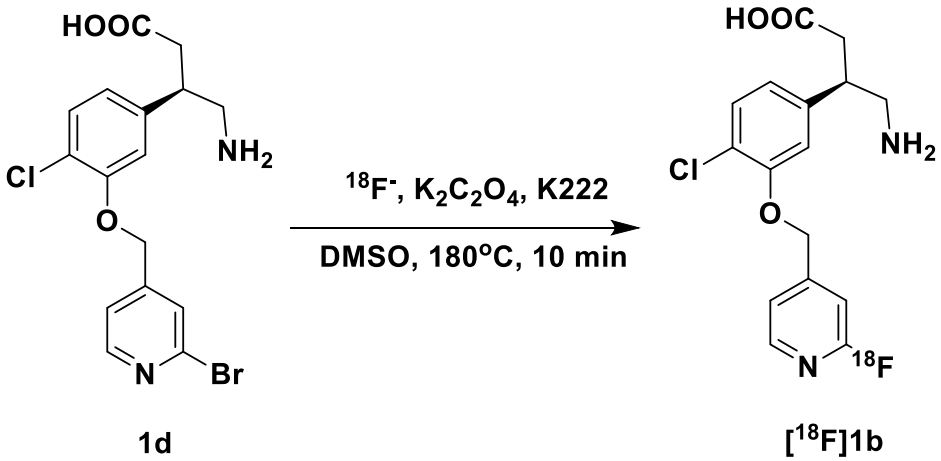

1d

[18F]1b